Light & Engineering
Vol. 28, No. 2, pp. 95–105, 2020

https://doi.org/10.33383/2019-021
Svetotekhnika #4, 2019, pp. 29–34

MAGNETIC FIELD IMPLEMENTING INTO THE ELECTROLUMINESCENCE OF OLED DEVICES DOPED WITH $CoFe_2O_4$ NANOPARTICLES

Selin Pıravadılı Mucur[1], Betül Canımkurbey[2], and Ayşe Demir Korkmaz[3]

[1]*The Scientific and Technological Research Council of Turkey (TÜBİTAK) Marmara Research Centre (MAM), Materials Institute, Kocaeli, Turkey*
[2]*Amasya University, Faculty of Arts and Sciences, Department of Physics, Amasya, Turkey*
[3]*Istanbul Medeniyet University, Faculty of Science, Department of Chemistry, Istanbul, Turkey*
E-mail: selin.piravadili@tubitak.gov.tr

ABSTRACT

Cobalt ferrite magnetic nanoparticles ($CoFe_2O_4$ MNPs) were successfully prepared by citric acid-assisted sol-gel auto combustion method and used in emissive layer of organic light emitting diode (OLED). Dimensional, structural and magnetic properties of $CoFe_2O_4$ nanoparticles (NPs) were recearched and compared by using X-ray diffraction (XRD), scanning electron microscopy (SEM), and vibrating sample magnetometer (VSM). $CoFe_2O_4$ MNPs were utilized at various concentrations (0.5 wt%, 1.0 wt% and 2.0 wt%) in the emissive layer of the OLEDs. The luminance, current efficiency and the electroluminescence characteristics of the devices with and without $CoFe_2O_4$ MNPs were investigated. An external magnetic field, B_{ext}, has also been applied to the OLEDs doped with MNPs while under operation. Effects of MNPs on OLED characteristics under B_{ext} were studied thoroughly. In the tailored device architecture, poly (3,4-ethylenedioxythiophene): poly polystyrene sulphonate (PEDOT: PSS) and poly(2-methoxy-5-(2-ethylhexyloxy))-1,4-phenylene vinylene (MEH-PPV) were used as a hole transport layer (HTL) and an emissive layer respectively with ITO/PEDOT: PSS/MEH-PPV: $CoFe_2O_4$/*Ca*/*Al* device architecture. The obtained results of the fabricated OLEDs were enhanced in the presence of $CoFe_2O_4$ NPs under B_{ext} due to providing density of states in the polymer matrices. The turn-on voltage was diminished slightly in the device doped with 0.5 % wt MNP compared to the devices with other concentrations of MNPs.

Keywords: magnetic field, OLED, electroluminescence, magnetic nano particles

1. INTRODUCTION

The field of organic devices that are based on π-conjugated organic materials has improved rapidly. At the moment, display and solid state lighting technology based on organic light emitting diodes (OLEDs) are the most immanent and developing field [1–3]. Although important progress has been achieved on the performance of OLEDs, further development is still needed for gaining a place in the market. Imbalanced charge injection, recombination and low fraction of singlet excitons limit the performances of devices [4, 5]. Using different charge injection and transport layers that have proper energy level or doping the charge transport and emissive layers are the recipe of controlling and balancing the carriers [4–8]. Device engineering and using nanomaterials are some examples to enhance OLED performance since radiative singlet excitons have a maximum value of 25 %, which is a restriction on efficiency of the device [5, 9–14]. Thus, there are various serious constraints for the development of OLEDs. Recently, experimental and theoretical studies have been performed which claim that the electron-hole recombination is spin de-

pendent [10, 15–21]. In particular, the recombination ratio is raised by the heavy atoms embedded in polymers [22]. Poly (*p*-phenylene vinylene) (PPV), polyfluorene (PFO), and their derivatives are the most frequently used polymers in device technology, but they have no heavy atoms in their backbone and 75 % triplet electron hole pair seriously limit the device efficiency. Therefore, the electroluminescence (EL) efficiency is enhanced by triplet electron hole pair conversion to the singlet exciton. Hu *et al.* used *CoPt* ferromagnetic nanowires in MEH-PPV and iridium complex *Ir* (ppy) to investigate the exciton formation [11]. When an external magnetic field is applied, *CoPt* nanowires increase the singlet-to-triplet exciton ratio in organic semiconductors that increase the singlet-to-triplet ratio. The doping of magnetic nanomaterials in OLEDs based on conjugated polymers has enhanced the performances [11, 14, 23]. Sun *et al.* doped $Co_{70}Fe_{30}$ MNPs in the emissive layer of OLEDs [23]. The EL of the device was enhanced with doping, and it was further enhanced when an external magnetic field was applied to the device. The increment in the fraction of singlet excitons and new trapping sites by magnetic field enhanced the generation of excitons. The pioneering studies were done in the discovery of magnetic field effects in organic semiconductors in 1960s [24–27]. Recently, the effects of magnetic field on tris (8-hydroxyquinoline) aluminum (III) (Alq_3) – based devices were searched by various groups [28–32]. The effect of magnetic field on organic semiconductors is explained by excitonic [33, 34] and bipolaron systems [35]. In the excitonic model, magnetic field changes intersystem conversion rates and traps the carriers in triplet state [33, 34]. In the bipolaron model, polarons were hopping and bipolarons were generated under magnetic fields [35].

Cobalt ferrite ($CoFe_2O_4$) is a kind of ferromagnetic materials. Recently, many academic and industrial studies have been done due to the magnetostrictive of $CoFe_2O_4$. Magnetostriction of a materials causes to change their shape or dimensions during the magnetization. This property has enabled applications in the surfaces on the wings of airplanes, sensors, corrosion in pipes. In this study, we reported and discussed the effects of $CoFe_2O_4$ MNPs doping in MEH-PPV. The hole transport studies in the MEH-PPV and MEH-PPV: $CoFe_2O_4$ MNPs composite have been carried out in ITO/PEDOT: PSS/MEH-PPV: $CoFe_2O_4$ MNPs/*Ca*/*Al* device configuration. Interesting results including applied B_{ext} have been found in these investigations. The doping of cobalt ferrite MNPs in MEH-PPV reduces the hole mobility by way of providing density of states (DOS), new trap sites and opened the way for balanced injection and radiative recombination of the charge carriers to realize improved performance of OLEDs. These results were reported and discussed in this study.

2. EXPERIMENT

2.1. Materials and Synthesis

All analytical grade chemicals for the synthesis, such as ferric nitrate nonahydrate ($(Fe(NO_3)_3 \cdot 9H_2O)$), cobalt nitrate tetrahydrate ($Co(NO_3)_2 \cdot 4H_2O$), citric acid and ammonia solution (30 %), were used without further purification. $CoFe_2O_4$ MNPs were synthesized as reported in the literature. Stoichiometric amounts of ferric nitrate and cobalt nitrate were dissolved in deionized water and poured into a crucible, in a molar ratio of 2:1. While this solution was being stirred, 2 g of citric acid to facilitate the distribution of the metal salts homogeneously and segregation of the metal ions was added [36]. Then, the pH was adjusted to 7.5 by adding ammonia to the solution in the crucible drop by drop. The solution was heated firstly to form a viscous gel and when the temperature reached to around 150 °C, a self-propagating combustion process occurred and a grey-black powder was obtained.

2.2. Instrumentation

The ITO-coated glass substrates (ITO thickness 120nm, 10 ohms/sq.) were purchased from KINTEC Systems Ltd. Aluminum (*Al*) pellets and *Ca* (99.99 % pure) was purchased from Kurt J. Lesker Company. PEDOT: PSS and MEH-PPV (Mn~40.000–70.000) were purchased from Heraeus Clevios GmbH and Sigma-Aldrich respectively. PEDOT: PSS was filtered through a 0.45 μm membrane PVDF filter. The MEH-PPV solution was prepared in toluene:1.2-dichlorobenzene (3:1) mixture with 8 mg/cm^3 concentration and filtered through a 0.45 μm PTFE membrane filter. $CoFe_2O_4$ powder was distributed in butyl benzoate at 8 mg/ml and the mixture was stirred for 2 hours by using ultrasonication. Patterned ITO-coated glass substrates were cleaned ultrasonically in acetone, detergent solution

(PCC-54 2 % wt dispersed in H_2O) and finally with deionized water and isopropyl alcohol respectively. Except for HTL, all device layers were deposited in a glove-box system.

Hamamatsu PMA-12 C10027 Photonic Multichannel analyzer and digital multimeter (2427-C3A Keithley) were used to measure electroluminescence, current efficiency, brightness and current-voltage relation of the devices with various MNPs concentration. All devices were measured in a dark sample chamber to get away any influence of ambient light. A stylus profiler (KLA Tencor P-6) was used to determine the thickness of organic layers. The optical transmission spectra were recorded using FS5 spectrofluorometer (Edinburg Inst, wavelength range of (300–800) nm. SEM images were acquired by a Philips XL 30 SFEG. Elemental distribution and associated spectra were obtained by EDAX Energy Dispersive X-ray Spectroscopy (EDS). Electron Spin Resonance spectrum was measured by Bruker ELEXSYS E580. The magnetic characterization was performed at room temperature by using a vibrating sample magnetometer (LDJ Electronics Inc., Model 9600) in an external field up to 15 kOe. The crystalline structure of the MNPs was determined with X-ray diffraction (XRD) measurements by using a Bruker D8 DISCOVER with DAVINCI design using *Cu Kα* radiation in the 2θ range of 20°–70°. Spin casting of the emissive layer was done within a controlled N2 environment in the glove-box system. All the devices of this study were exposed to air after the encapsulation with epoxy under UV light for 3 minutes.

2.3. Device Fabrication

PEDOT: PSS was used as for the holes injection layer (HIL). A layer of PEDOT: PSS (thickness ~ 60 nm) was spin-coated onto the pre-cleaned ITO-coated glass at 4000 rpm for 30 s and then baked at 120 °C for 20 min. This procedure flattens the ITO-coated glass slides, gets rid of humidity from surface and avoids short circuits. $CoFe_2O_4$ MNPs: MEH-PPV blend was prepared in the concentration of 0.5 % wt, 1.0 % wt and 2.0 % wt. This blend was deposited (thickness ~ 100 nm) on top of the holes injection layer by spin coating at 1000 rpm for 40 s then baked at under its T_g for 20 min in N_2 environment to evaporate the solvents. Finally, calcium as an electron injection layer (~15 nm) and cathode layer of aluminium (~120 nm) were deposited by vacuum evaporation (5 x 10^{-6} mbar) technique. The active emission area was 9.0 mm^2. The thickness of evaporated layers was measured by a quartz crystal monitor. The devices with ITO/PEDOT: PSS/MNPs: MEH-PPV/*Ca*/*Al* structure were fabricated.

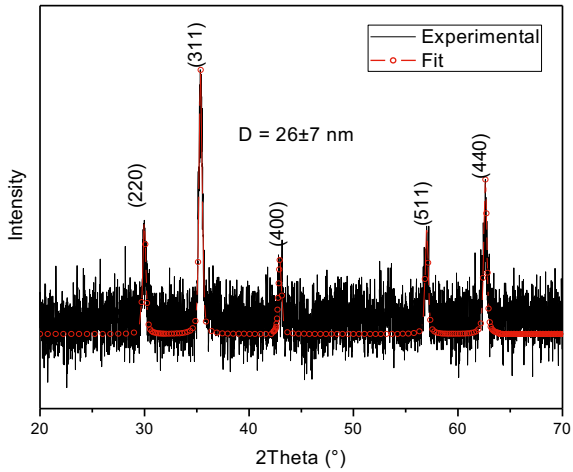

Fig. 1. XRD powder pattern of $CoFe_2O_4$ MNPs.

3. RESULTS AND DISCUSSION

3.1. XRD Analysis of $CoFe_2O_4$ MNPs

The structure and phase purity of $CoFe_2O_4$ MNPs were confirmed by investigating their X-ray diffraction pattern as seen in Fig. 1. All the observed XRD peaks could be assigned to cubic spinel lattice indicating the single phase cubic spinel structure of $CoFe_2O_4$ MNPs. The broadening of the peaks was due to the small crystallite size. The line profile fitting technique stated in Wejrzanowski *et al.* [37, 38] was applied by fitting five observed peaks of the XRD powder pattern with the following miller indices: (220), (311), (400), (511) and (440) to calculate the mean size of the crystallites. The peaks matched very well with the Powder Diffraction File (PDF) card number 00–022–1086. The line profile fitting method revealed that the mean crystallite size was 26±7 nm.

3.2. SEM Analysis of $CoFe_2O_4$ NPs

The particle morphologies of the $CoFe_2O_4$ MNPs were investigated using SEM micrographs. The surface of the $CoFe_2O_4$ MNPs composed of platelets as seen in Fig 2b. The platelet like structure was also observed in a study by Venkatesan *et al.*

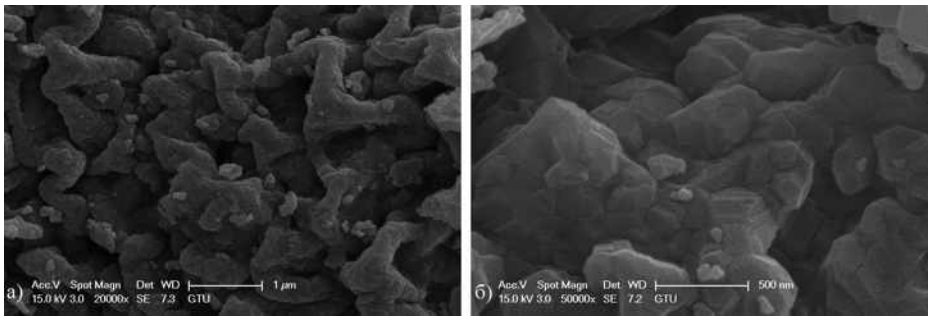

Fig. 2. SEM analysis of $CoFe_2O_4$ MNPs

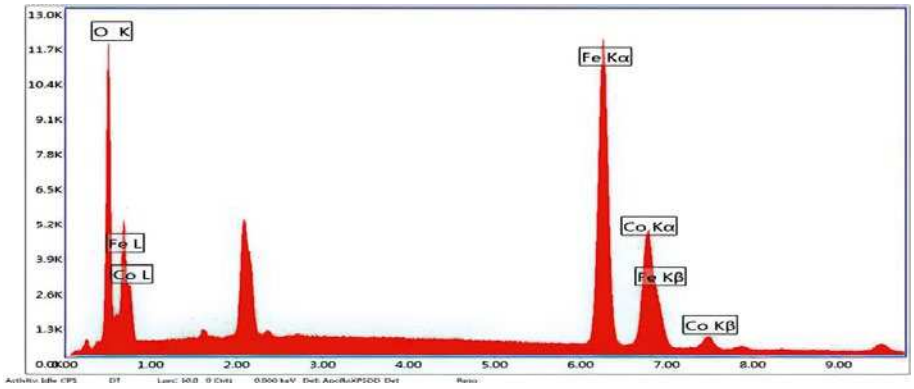

Fig. 3. Elemental distribution and associated spectra were obtained by EDAX Energy Dispersive X-ray Spectroscopy (EDS) of $CoFe_2O_4$ MNPs coated with gold

where $CoFe_2O_4$ MNPs were synthesized by solution combustion method. They suggested that the formation of agglomerated particles was due to less gas being released during the combustion process [39]. The SEM analysis showed the agglomeration of particles which might also be due to the magnetic attraction of nanoparticles to each other.

In order to confirm the presence and the composition of cobalt ferrite nanoparticles, the final product was characterized by energy dispersive spectroscopy (EDS) coupled with SEM unit. EDS scan supported the presence of $CoFe_2O_4$ with the inclusion of cobalt, oxygen, cobalt, and iron respectively. No impurity was detected in the synthesized $CoFe_2O_4$ MNPs. A profile of these four elements was shown in Fig. 3.

3.3. VSM Analysis of $CoFe_2O_4$ NPs

The magnetization of the $CoFe_2O_4$ MNPs has been studied as a function of the applied magnetic field using a variable sample magnetometer (VSM) at 300 K and the behaviour was shown in Fig. 4. The hysteresis loop of magnetization indicated the ferromagnetic behaviour of $CoFe_2O_4$ MNPs. The field dependent magnetization (M-H) curve of $CoFe_2O_4$ MNPs was recorded at room temperature by varying the externally applied field up to ±15 kOe. The saturation magnetization (σ_s) value was determined

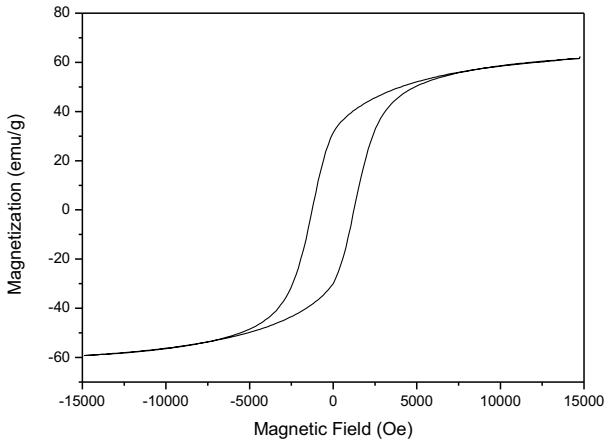

Fig. 4. The magnetization of the $CoFe_2O_4$ MNPs as a function of the applied magnetic field using a variable sample magnetometer (VSM) at 300 K

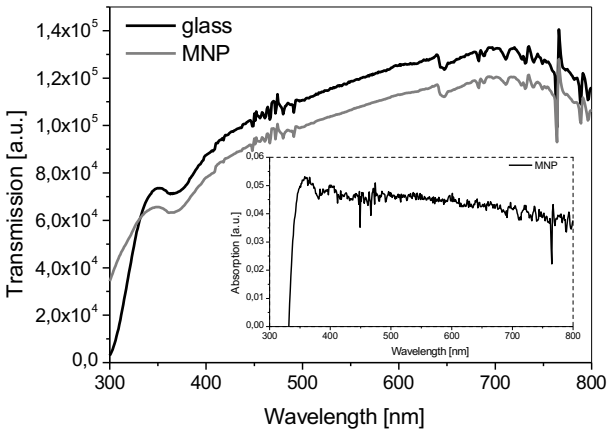

Fig. 5. Transmission and absorption properties of the MNP thin film

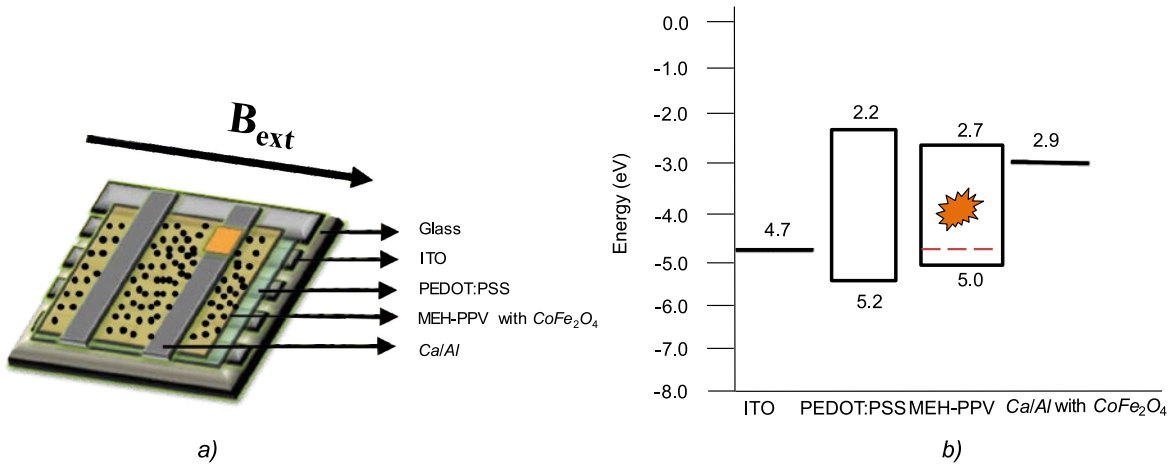

Fig. 6. Schematic cross-sectional structure of OLED and chemical structure of polymer used in this study – a; energy diagram of the OLED: the highest occupied molecular orbital (HOMO) and lowest unoccupied molecular orbital (LUMO) band energies – b

by the law of as approaching saturation, which is also known as the Stoner-Wohlfarth (S-W) model by extrapolating the plot of σ (magnetization) vs $1/H^2$ to, where $1/H^2$ approaches zero [40]. The S-W model accounts for single-domain and non-interacting particles carrying randomly oriented uniaxial anisotropy directions [41]. Based on the S-W model mentioned above, the maximum saturation magnetization value (M_s) was determined as 60.78 emu·g^{-1} lower than the 80.8 emu·g^{-1} value M_s for bulk $CoFe_2O_4$ [42]. The remnant magnetization (Mr) was found as 30.69 emu·g^{-1} and the coercivity (Hc) was determined as 1246 Oe, which was somewhat smaller than that of bulk $CoFe_2O_4$ with a room-temperature coercivity of 5.4 kOe [43]. These results might be arising from a spin-glass shell formed as the magnetically dead or inert layer on the surface of cobalt ferrite nanoparticles [42, 43].

The remanence (M_r) to saturation (M_s) magnetization ratio (M_r/M_s) was found to be 0.50 which was expected for a system with non-interacting single-domain particles with uniaxial anisotropy directions [44, 45].

3.4. Photophysical Properties of $CoFe_2O_4$ NPs

The photo-physical properties of $CoFe_2O_4$ MNPs in butyl benzoate thin film, which were spin coated on glass substrates, were investigated by UV–VIS absorption, Fig. 5. A little absorption behaviour was observed and correspondingly, transmission values were nearly the same with glass substrates. This high transmission characteristics allow the use of MNPs in OLED devices.

3.5. Electroluminescence Properties

Fabricated OLED device structure could be seen from Fig. 6a. Fabrication procedure was discussed in detailed in experimental section. It was clearly seen from Fig. 6b that the HOMO energy level of MEH-PPV polymer matched with the PEDOT: PSS HOMO energy level, thus the transportation of holes from ITO to emissive layer becomes easier. MEH-PPV has also suitable lowest unoccupied molecular orbital (LUMO) energy level (–2.75 eV), which is high enough to transport of electrons from the cathode, thus this improved the luminance efficiency by efficient recombination of electrons and holes in the emissive layer. The Fermi level of the doped $CoFe_2O_4$ MNPs was ~0.3 eV lower than the HOMO of MEH-PPV. Similar to the doping of single wall carbon nano-tubes in polymers [11, 14], it might be derived that in this case, also the holes may get injected into MNPs and transport via internal hopping through MNPs. To investigate the effect of the concentration of $CoFe_2O_4$ MNPs on the OLED device performances, the emissive layer was doped with $CoFe_2O_4$ MNPs in various concentrations: 0.5 % wt, 1.0 % wt and 2.0 % wt.

All the devices exhibited the same luminance values, Fig. 7a, while the device doped with 0.5 % MNPs had maximum luminous efficiency and EQE, 0.83 cd/A and 0.43 % respectively, Fig. 7b and Fig. 7d. The device characteristics were enhanced upon varied concentrations of MNPs as summarized in Table 1. **Fig. 7c** showed the experimental I–V characteristics of the devices at different MNP concentrations. The turn-on voltage values of the de-

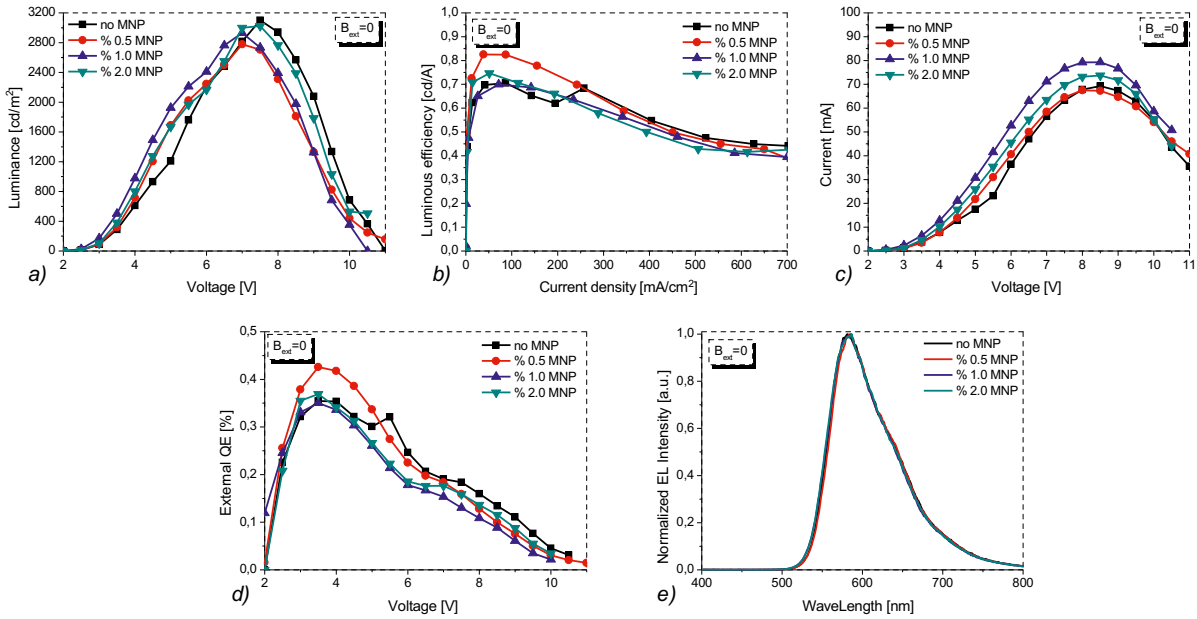

Fig. 7. OLED characteristics for different MNPs concentration: a) luminance–voltage, b) luminous efficiency–current density, c) current–voltage, d) EQE- voltage, e) normalized EL intensity

vices were slightly different. The conductance and charge hopping mechanism of the devices including MNPs were expected to increase their charge carrying mobility and resulted in lower turn-on voltages. In this study, the devices with doped MNPs showed lower turn-on voltage compared with the device without MNPs. The device turn-on voltage for the emission of photons is associated with the minority carrier injection. At low voltages, I–V characteristics showed Ohmic behaviour. At higher voltages, I–V behaviour was found to be governed by space charge limited conduction (SCLC). In the SCLC, current has directly proportional with the density of states (DOS).

As it could be seen in the Fig. 7c, the current of the devices with MNPs were higher than the device without MNPs, therefore doping concentration could increase the DOS. However, due to the small size and low concentration of the particles in the present case, the MNPs did not form local conducting channels as in the case of nano-rods. Further, as the MNPs were distributed homogenously throughout the MEH-PPV layer, the probability of internal hopping through the particles was negligible. Therefore, the most probable way was each nanoparticle served as a trap for the holes. Therefore, the trap density was being enhanced by the doping of MNPs in MEH-PPV. Note that the enhancement in the net trap density in the blend did not exactly correspond to the nanoparticle density. The increment in the trapping sites was more than the density of the MNPs in the present case. In general, the traps were created in a system by the doping/impurities and the structural/interfacial defects [42]. When MNPs were doped in emissive layer interface defect states at the MEH-PPV–MNPs interface were also created, which could serve as trapping sites; therefore, the number of trapping sites increased more than the density of the MNPs. It was also important to note that because of low doping and good dispersion of MNPs, we have ruled out the possibility of formation of conducting channels and particle–particle interaction in the present case. However, particle–particle interaction can play an important role in the determination of device performance. Bakuzis *et al*. [43] investigated particle–particle interaction in magnetic fluids containing MNPs. The interaction of the particles depends on their concentration. The higher the particle concentration the lower the particle–particle distance, which increases the interaction among the nanoparticles.

The EL spectra of the fabricated OLEDs were shown in Fig. 7e. EL spectrum exhibited peak is about 594 nm wavelength. All devices had EL emission peak at the same wavelength, namely MNPs did not affect the morphology and dominant wavelength of the emitted light from OLEDs.

These *J-V* curves were described by a power law of $J \sim V^{m+1}$ and, in logarithmic scale (Fig. 8) to determine the mechanisms of electrical conductivi-

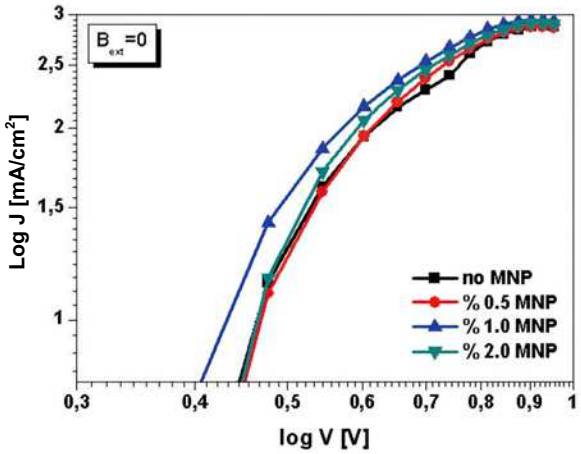

Fig. 8. Logarithmic dependencies of current density-voltage curves

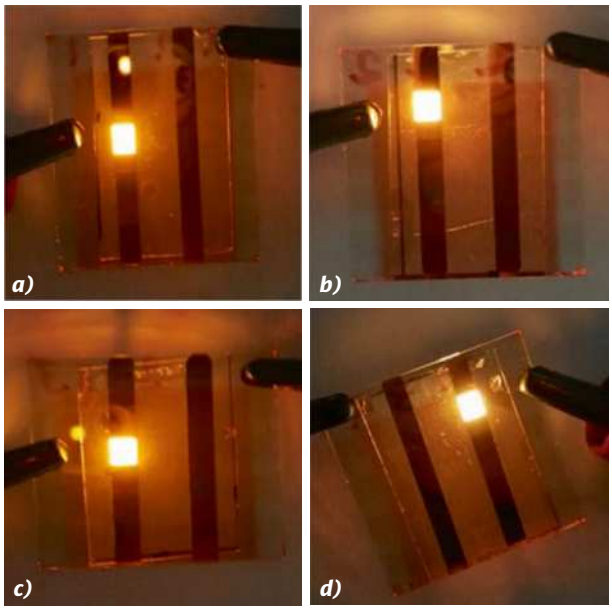

Fig. 9.The light output at 6 V of OLEDs with a) no MNP, b) 0.5 % wt, c) 1.0 % wt, d) 2.0 % wt

ty of the devices. At the low voltage area, the conduction mechanism is given by m = 1 in all devices, therefore, this behaviour can show the hole current contribution as a space charge limited conduction (SCLC) mode with no traps, given by:

$$J=9/8(\varepsilon_0\varepsilon_r)\mu V^2L^{-3},$$

where μ is the carrier mobility, $\varepsilon_0\varepsilon_r$ is the permittivity of MEH-PPV and L is the thickness of the sample. At the high voltage area, decrease of the current density can be observed suggesting a trap distribution where the electrons were trapped mainly by the MNP, which were filled during the charge injection in the OLEDs. In the absence of oxidizing mechanism on the surfaces, the MNP should favoured the hole injection inducing the lowering of the critical voltage because the Fermi level of MNP was between that of the ITO and the HOMO level of the emission layer.

In Fig. 9, the light output images of the OLEDs with varied MNPs concentration could be seen under applied voltage 6 V. In Fig. 10, the performanc-

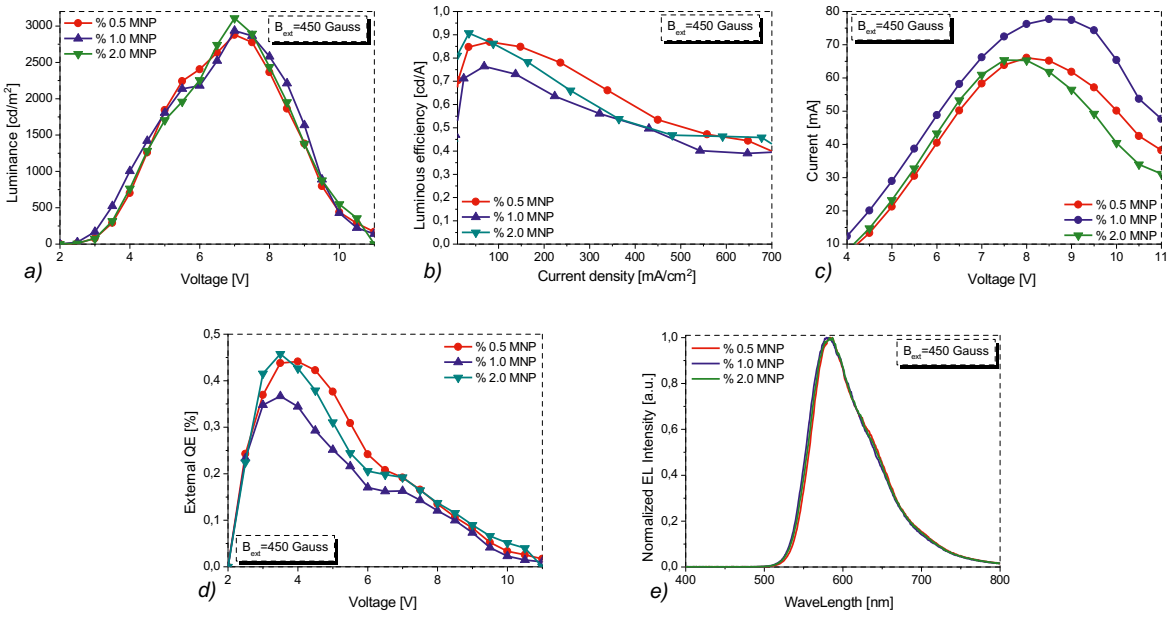

Fig. 10. The performances of the devices with MNPs under B_{ext}: a) luminance–voltage, b) luminous efficiency–voltage, c) current–voltage, d) EQE- voltage, e) normalized EL intensity

Table 1. Device Performances of OLEDs Depending on MNP Concentrations in the Emissive Layer with / without Applied Magnetic Field (B_{ext})

Device Configuration	Turn on Voltage* [V]	Max. Luminance [cd/m^2]	Max.Luminous Efficiency [cd/A]	EQE [%]
B_{ext}=0				
No MNP	2.05	3101	0.71	0.35
0.5 % wt MNP	2.04	2279±2.5	0.83±0.03	0.43±0.01
1.0 % wt MNP	2.01	2931±5.7	0.70±0.01	0.35±0.04
2.0 % wt MNP	2.04	3023±6.3	0.75±0.07	0.37±0.04
$B_{ext}\neq0$				
0.5 % wt MNP	1.72	2879±0.5	0.87±0.02	0.44±0.03
1.0 % wt MNP	2.02	2935±5.7	0.76±0.09	0.37±0.08
2.0 % wt MNP	2.06	3108±8.8	0.91±0.10	0.47±0.04

*Turn on voltage is defined as the applied voltages when the luminance is 1 cd/m^2.
Each error was found between the pixels of the same device.

es of the devices with MNPs could be seen under B_{ext}. In our study, a 45 mT (450 Gauss) homogenous magnetic field was applied to the doped devices under operation. The values were also summarized at the Table 1. As seen in the Table 1**,** the performances of all MNPs doped devices under B_{ext} were enhanced. As an example, the luminance of the device doped with 0.5 % MNPs increased from 2279 cd/m^2 up to 2879 cd/m^2 while luminous efficiency increased from 0.83 cd/A to 0.87 cd/A respectively. This device had also the lowest turn-on voltage among all devices (Fig. 7). These investigations could be applied for other MNP-doped devices. Early studies demonstrated that magnetic fields can influence the triplet-triplet annihilation process in organic materials and can change the intensity of the resulting delayed fluorescence signal. Additionally, it was found that magnetic fields also have an effect on the photoconductivity of organic films. Finally, a broad interest in magnetic phenomena in organics started to arise when the magnetic field effect on device current and electroluminescent properties of OLED devices was discovered [48–50]. In 2003, Kalinowski *et al.* discovered that in tri-(8-hydroxyquinoline)-aluminium (Alq_3) based devices with non-magnetic electrode materials the application of a magnetic field of 500 mT increases the current flow through the devices as well as their light output by up to 3 % [29]. This novel phenomenon started to receive increasing attention one year later when Francis et al. demonstrated that a large change in the resistance of more than 10 % can be succeeded in polyfluorene based OLEDs at room temperature and weak magnetic fields in the order of 10 mT [31]. This publication introduced the term "organic magnetoresistance effect" (OMR effect) and triggered several studies in the following years. Mermer et al. showed that the OMR effect is a general phenomenon and can be observed in both polymeric and small-molecule materials [32, 50, 51]. Therefore, the enhancement in the device performances might be attributed to the delayed fluorescence phenomenon because of triplet-triplet annihilation, so the singlet state is formed in the system. The EL spectra of the fabricated OLEDs were shown in Fig. 10 e. EL spectrum exhibited a peak at ~ 594 nm, the same as with B_{ext} = 0. Therefore, the application of B_{ext} did not have an influence on the emitted light characteristics but enhanced the performance of the devices. Desai *et al.* have been observed that low magnetic field can increase the triplet concentration due to an increase in the rate of intersystem crossing from photo-generated singlet to triplet state [44]. When the number of triplet excitons increase, due to longer lifetime of triplet excitons compared to that of the singlet excitons in bulk materials, dissociated charge carriers can increase. Applied magnetic field increases the intersystem crossing rate leading to an increase in the triplet population, which in turn increases the efficiency.

4. CONCLUSION

In this work, we presented the effect of concentration of MNPs on the performance of OLEDs under B_{ext}. In conclusion, $CoFe_2O_4$ MNPs were doped in MEH-PPV and device characteristics were carried out at different concentrations under applied magnetic field. Doping of MNPs in MEH-PPV had no effect on EL characteristics but increased DOS. Device performances with MNPs were enhanced under applied B_{ext} when the device was under operation. This was an important fundamental and applied finding that could help in achieving balanced radiative recombination of the charge carriers and hence improved performances in OLEDs.

5. REFERENCES

1. A. Köhler, J.S. Wilson, R.H. Friend, Fluorescence and phosphorescence in organic materials// Advanced Engineering Materials, 2002, Vol. 4, #7, 453p.

2. B.W. D'Andrade, S.R. Forrest, White organic light emitting devices for solid state lighting// Advanced Materials, 2004, Vol. 16, #18, pp. 1585–1595.

3. J. Feng, T. Okamoto, R. Naraoka, S. Kawata, Enhancement of surface plasmon-mediated radiative energy transfer through a corrugated metal cathode in organic light-emitting devices// Applied Physics Letters, 2008, Vol. 93, #5, 051106.

4. T. Ahn, H. Lee, S.-H. Han, Effect of annealing of polythiophene derivative for polymer light-emitting diodes// Applied physics letters, Vol. 80, #3, pp. 392–394.

5. A. Misra, P. Kumar, M. Kamalasanan, S. Chandra, White organic LEDs and their recent advancements// Semiconductor science and Technology, 2006, Vol 21, #7, R35.

6. S.-M. Seo, J.H. Kim, J.-Y. Park, H.H. Lee, Coordination-complex polymer as an organic conductor for organic light-emitting diodes// Applied Physics Letters, Vol. 87, #18,183503.

7. S.Y. Kim, J.M. Baik, H.K. Yu, K.Y. Kim, Y.-H. Tak, J.-L. Lee, Rhodium-oxide-coated indium tin oxide for enhancement of hole injection in organic light emitting diodes// Applied Physics Letters, 2005, Vol. 87, #7, 072105.

8. J.-H. Li, J. Huang, Y. Yang, Improved hole-injection contact for top-emitting polymeric diodes// Applied physics letters,2007, Vol. 90, #17, 173505.

9. M. Suzuki, S. Tokito, F. Sato, T. Igarashi, K. Kondo, T. Koyama, T. Yamaguchi, Highly efficient polymer light-emitting devices using ambipolar phosphorescent polymers// Applied Physics Letters, 2005, Vol. 86, #10, 103507.

10. M. Baldo, D. O'brien, M. Thompson, S. Forrest, Excitonic singlet-triplet ratio in a semiconducting organic thin film// 1999, Physical Review B, Vol. 60, #20, 14422.

11. B. Hu, Y. Wu, Z. Zhang, S. Dai, J. Shen, Effects of ferromagnetic nanowires on singlet and triplet exciton fractions in fluorescent and phosphorescent organic semiconductors// Applied physics letters, Vol. 88, #2, 022114.

12. P.P. Ruden, D.L. Smith, Theory of spin injection into conjugated organic semiconductors// Journal of applied physics, 2004, Vol. 95, #9, pp. 4898–4904.

13. P. Blom, M. De Jong, S. Breedijk, Temperature dependent electron-hole recombination in polymer light-emitting diodes// Applied Physics Letters,1997, Vol. 71, #7, pp. 930–932.

14. Z. Xu, Y. Wu, B. Hu, I.N. Ivanov, D.B. Geohegan, Carbon nanotube effects on electroluminescence and photovoltaic response in conjugated polymers// Applied Physics Letters, 2005, Vol. 87, #26, 263118.

15. Y. Cao, I.D. Parker, G. Yu, C. Zhang, A.J. Heeger, Improved quantum efficiency for electroluminescence in semiconducting polymers// Nature,1999, Vol. 397, #6718, pp. 414–417.

16. P.K. Ho, J.-S. Kim, J.H. Burroughes, H. Becker, S.F. Li, T.M. Brown, F. Cacialli, R.H. Friend, Molecular-scale interface engineering for polymer light-emitting diodes// Nature, 2000, Vol. 404, #6777, pp. 481–484.

17. M. Wohlgenannt, K. Tandon, S. Mazumdar, S. Ramasesha, Z. Vardeny, Formation cross-sections of singlet and triplet excitons in π-conjugated polymers// Nature, 2001, Vol. 409, #6819, pp. 494–497.

18. J. Wilson, A. Dhoot, A. Seeley, M. Khan, A. Köhler, R. Friend, Spin-dependent exciton formation in π-conjugated compounds// Nature, 2001, Vol. 413, #6858, pp. 828–831.

19. Z. Shuai, D. Beljonne, R. Silbey, J.-L. Brédas, Singlet and triplet exciton formation rates in conjugated polymer light-emitting diodes// Physical review letters, 2000, Vol. 84, #1, 131.

20. M.N. Kobrak, E.R. Bittner, Quantum molecular dynamics study of polaron recombination in conjugated polymers// Physical Review B, 2000, Vol. 62, #17, 11473.

21. T.-M. Hong, Meng H.-F. Spin-dependent recombination and electroluminescence quantum yield in conjugated polymers// Physical Review B, 2001, Vol. 63, #7, 075206.

22. V. Cleave, G. Yahioglu, P.L. Barny, R.H. Friend, Tessler N. Harvesting singlet and triplet energy in polymer LEDs// Advanced Materials, 1999, Vol. 11, #4, pp. 285–288.

23. C.-J. Sun, Y. Wu, Z. Xu, B. Hu, J. Bai, J.-P. Wang, Shen J. Enhancement of quantum efficiency of organic light emitting devices by doping magnetic nanoparticles// Applied physics letters, 2007, Vol. 90, #23, 232110.

24. E.L. Frankevich, Balabanov E.L. New effect of increasing the photoconductivity of organic semiconductors in a weak magnetic field// ZhETF Pisma Redaktsiiu, 1965, Vol. 1, #6, pp. 33–37.

25. E. Frankevich, The nature of a new effect of a change in the photoconductivity of organic semiconductors in a magnetic field, Soviet Physics JETP// 1966, Vol. 23, #5, pp. 1226–1234.

26. E.L. Frankevich, E.L. Balabanov, Changes in photoconductivity of an anthracene single crystal in amagnetic field// Solid State Physics, 1966, Vol. 8, #3, pp. 855–889.

27. E. Frankevich, E.L. Balabanov, G.V. Vselyubskaya, Investigation of change in photoconductivity of organic semiconductors in a magnetic field//Solid State Physics, 1966, Vol. 8, pp. 1970–1973.

28. J. Kalinowski, J. Szmytkowski, Stampor W. Magnetic hyperfine modulation of charge photogeneration in solid films of Alq 3// Chemical physics letters, 2003, Vol. 378, #3, pp. 380–387.

29. J. Kalinowski, M. Cocchi, D. Virgili, P. Di Marco, Fattori V. Magnetic field effects on emission and current in Alq 3-based electroluminescent diodes// Chemical Physics Letters, 2003, Vol. 380, #5, pp. 710–715.

30. A.H. Davis, Bussmann K. Large magnetic field effects in organic light emitting diodes based on tris (8-hydroxyquinoline aluminum)(Alq 3)/N, N′-Di (naphthalen-1-yl)-N, N′ diphenyl-benzidine (NPB) bilayers// Journal of Vacuum Science & Technology A: Vacuum, Surfaces, and Films, 2004, Vol. 22, #4, pp. 1885–1891.

31. T. Francis, Ö. Mermer, G. Veeraraghavan, Wohlgenannt M. Large magnetoresistance at room temperature in semiconducting polymer sandwich devices// New Journal of Physics, 2004, Vol. 6, #1, 185.

32. Ö. Mermer, G. Veeraraghavan, T. Francis, Y. Sheng, D. Nguyen, M. Wohlgenannt, A. Köhler, M.K. Al-Suti, Khan M., Large magnetoresistance in nonmagnetic π-conjugated semiconductor thin film devices// Physical Review B, 2005, Vol. 72, #20, 205202.

33. V. Prigodin, J. Bergeson, D. Lincoln, Epstein A. Anomalous room temperature magnetoresistance in organic semiconductors// Synthetic Metals,2006, Vol. 156, #9, pp. 757–761.

34. P. Desai, P. Shakya, T. Kreouzis, W. Gillin, N. Morley, Gibbs M. Magnetoresistance and efficiency measurements of Al q 3-based OLEDs// Physical Review B, Vol. 75, #9, 094423.

35. P. Bobbert, T. Nguyen, F. Van Oost, V.B. Koopmans, Wohlgenannt M. Bipolaron mechanism for organic magnetoresistance// Physical Review Letters, 2007, Vol. 99, #21216801.

36. H. Kavas, A. Baykal, A. Demir, M.S. Toprak, Aktaş B. ZnxCu (1– x) Fe_2O_4 Nanoferrites by Sol–Gel Auto Combustion Route: Cation Distribution and Microwave Absorption Properties// Journal of Inorganic and Organometallic Polymers and Materials, 2014, Vol. 24, #6, pp. 963–970.

37. Pielaszek R. Analytical expression for diffraction line profile for polydispersive powders, Applied Crystallography// Proceedings of the XIX Conference, World Scientific, Singapore, 2004, pp. 43–50.

38. T. Wejrzanowski, R. Pielaszek, A. Opalińska, H. Matysiak, W. Łojkowski, Kurzydłowski K. Quantitative methods for nanopowders characterization// Applied Surface Science, 2006, Vol. 253, #1, pp. 204–208.

39. K. Venkatesan, D.R. Babu, M.P.K. Bai, R. Supriya, R. Vidya, S. Madeswaran, P. Anandan, M. Arivanandhan, Hayakawa Y. Structural and magnetic properties of cobalt-doped iron oxide nanoparticles prepared by solution combustion method for biomedical applications// International journal of nanomedicine, 2015, Vol. 10, Suppl 1, 189.

40. S. Asiri, S. Güner, A. Demir, A. Yildiz, A. Manikandan, Baykal A. Synthesis and Magnetic Characterization of Cu Substituted Barium Hexaferrites// Journal of Inorganic and Organometallic Polymers and Materials, 2018, Vol. 28, #3, pp. 1065–1071.

41. Kojima H. Fundamental properties of hexagonal ferrites with magnetoplumbite structure// Handbook of Ferromagnetic Materials, 1982, 3, pp. 305–391.

42. K.C. Kao, Hwang W., Electrical transport in solids, wuth particular reference to orgainc semiconductorys// Pergamon Press, 1981.

43. A. Bakuzis, A. Pereira, J. Santos, Morais P. Superexchange coupling on oleylsarcosine-coated magnetite nanoparticles// Journal of Applied Physics, 2006, Vol. 99, #8, 08C301.

44. P. Desai, P. Shakya, T. Kreouzis, Gillin W.P. The role of magnetic fields on the transport and efficiency of aluminum tris(8-hydroxyquinoline) based organic light emitting diodes// Journal of Applied Physics, 2007, Vol. 102, #7, 073710.

Selin Piravadili Mucur
after completing her primary and secondary education in Bandırma completed her graduate and Master of Science education at Hacettepe University in Physics Engineering Department in period 2000–2007. In 2011, she began experimental studies as a student in the Photonics, Electronics and Sensors Laboratory TÜBİTAK UME and started her Ph.D. program in the Institute of Engineering and Science, Physics Department at Gebze Technichal University and finished it in 2015. Her Ph.D. subject was "Effect of Metal and Semiconductor Nanoparticles on the Performance of Organic Lıght Emitting Diodes Based on Conjugated Polymers". Since 2013, she has been working as a researcher in the Photonics Technologies Group at Marmara Research Centre, TUBITAK. Her scientific field interests are optoelectronic devices, organic field effect transistors, thin films, organic light emitting devices, and organic photovoltaic devices

Betül Canimkurbey
has graduated from Gebze Technical University with Ph.D. degree in 2017. At present, she is an Assistant Professor and the Assistant Director of the central research laboratory at Amasya University. Her scientific field interests are: optoelectronic devices, organic field effect transistors, thin films, organic light emitting devices, and organic photovoltaic devices

Ayse Demir Korkmaz
received her Ph.D. degree in chemistry from Fatih University in Istanbul, Turkey in 2015. She has been working as a research assistant in Istanbul Medeniyet University since 2012 where she conducts research activities in the areas of magnetic nanoparticles, inorganic nanomaterials, and their biomedical applications